

# BENZAMIDE SPECIES RETAINED BY DMSO COMPOSITES AT A KAOLINITE SURFACE

B. Caglar, B. Afsin\* and A. Tabak

Department of Chemistry, Faculty of Arts and Sciences, Ondokuz Mayıs University, Kurupelit, Samsun, 55139 Turkey

The surface area of kaolinite-benzamide (K-Bz)  $6.62 \text{ m}^2 \text{ g}^{-1}$ , which is noticeably lower than that of kaolinite-dimethyl sulphoxide (K-DMSO)  $14.61 \text{ m}^2 \text{ g}^{-1}$ , the co-perturbation of the inner-surface hydroxyl features at  $3697$  and  $3650 \text{ cm}^{-1}$ , and the increase of  $d(001)$  value by  $7.44 \text{ \AA}$  are all related to the benzamide species inserted into the kaolinite structure through the replacement of the K-DMSO composites. Disappearance of the DMSO reflections and emergence of well-defined features at  $6.04(2\theta)$  and  $11.16(2\theta)$ ,  $001$  and  $002$  reflections with  $d$  values of  $14.62$  and  $7.92 \text{ \AA}$ , respectively point out that the DMSO species were substituted efficiently by benzamide molecules. The thermal stability of the K-Bz derivative up to  $300^\circ\text{C}$  can be attributed to the slightly tilted aromatic ring keying into the gibbsitic sheets via the  $-\text{NH}_2$  groups.

**Keywords:** benzamide, DMSO, inner surface hydroxyls, kaolinite, preadsorption

## Introduction

Surface processes of modest size aromatic molecules on clay matrices have been of massive interest for elucidating the chemical reactivity and mechanical properties of organo-clay composites [1–3]. The organo-clay composites which possess large specific surface area, considerable porosity and thermal stability have been widely used in a range of key processes as ion exchangers, selective adsorbents and reinforcing fillers for plastics and electric materials [4–6]. The host centres produced by immobilization of specific guest molecules such as formamide, urea and short chain oil acids through strong hydrogen bonds into the inorganic matrices such as kaolinite are of great importance in catalysis [7–10]. Organic and inorganic molecules may form ‘intercalation compounds’ within the unique structure of kaolinite by overcoming the cohesive forces between free surface hydroxyl groups [11] whereas non-reacting molecules of large size are entrained by the precursors such as DMSO and NMF [7, 12]. Considerable attention has been paid to characterize the precursors to ordered organo-clay composites formed on kaolinite-type minerals [13–15].

The benzamide species retained by pre-adsorbed DMSO composites at a kaolinite surface which should represent a clear possibility of new and promising materials were examined in present work through the use of FTIR, thermal analysis (TG-DTG and DTA), X-ray powder diffraction (XRD) and surface area measurement techniques.

## Experimental

XRD pattern of the kaolinite (K, Sigma,  $212 \mu\text{m}$ ) showed no crystalline impurities. DMSO [Fluka, 99.9%, (G.C.)] and benzamide (Fluka,  $\geq 98\%$  (UV)) were used as received. 3 g K was mechanically stirred with 40 mL DMSO at  $60^\circ\text{C}$  for 2 days in a 50-mL flat-bottomed glass flask and the resulting kaolinite-dimethyl sulphoxide (K-DMSO) composite was washed with ethanol two times; the supernatant solution was centrifuged at 2000 rpm and the solid product was dried for 2 days at  $60^\circ\text{C}$  to eliminate the excess of DMSO [13, 14]. The displacement technique (from the K-DMSO composite) was used to prepare the kaolinite-benzamide (K-Bz) intercalate. 1 g K-DMSO was thoroughly mixed with excess benzamide aqueous solution for 5 days at  $130^\circ\text{C}$ . The supernatant was discarded and the product washed twice with ethanol and subsequently by hot water. The solid product was dried for 2 days at  $80^\circ\text{C}$  and then sieved to  $212 \mu\text{m}$  [9].

XRD profiles were recorded on a Rigaku 2000 instrument using Ni-filtered  $\text{CuK}\alpha$  radiation ( $\lambda$ ,  $1.54050 \text{ \AA}$ ) at 40 kV and 40 mA. Infrared spectra were collected in the  $4000\text{--}200 \text{ cm}^{-1}$  region with Mattson-1000 FTIR spectrometer at  $4 \text{ cm}^{-1}$  resolution using KBr pellet technique.

Simultaneous TG-DTG and DTA curves were monitored using Rigaku TG 8110 analyser equipped with TAS 100 from room temperature to  $1000^\circ\text{C}$  at a heating rate of  $10^\circ\text{C min}^{-1}$  under nitrogen flow (calcinated  $\alpha$ -alumina was taken as the reference). Surface areas were measured by nitrogen adsorption at 77 K using Quantachromosorb.

\* Author for correspondence: bafsin@omu.edu.tr

## Results and discussion

Shown in Fig. 1a–b are the comparative FTIR spectra of nonintercalated and DMSO intercalated kaolinite samples. A careful examination of the spectra suggests that the sharp peaks at 3662, 3541 and 3504  $\text{cm}^{-1}$  are interrelated in that the recessed location of the inner hydroxyl groups accounts for the considerable intensity decrease of the 3697  $\text{cm}^{-1}$  band in parallel with the extent of intercalation. The low-frequency modes of the intercalated species which are suppressed by the intense peaks related to the framework of kaolinite complement the 3697 and 3650  $\text{cm}^{-1}$  stretches co-perturbed by the guest species. The reduced intensity of the 912 and 791  $\text{cm}^{-1}$  peaks prove clearly that, of different hydroxyls, the ‘inner-sheet hydroxyls’ contributed most to the hydrogen bonding directly with the DMSO intercalates embedded in the gallery space of kaolinite [7, 11, 16]. The upward and downward shifts of the asymmetric and symmetric C–H stretches of pure DMSO at 2994 and 2993  $\text{cm}^{-1}$  to 3022 and 2937  $\text{cm}^{-1}$ , respectively are seen as an outcome of the interaction of methyl groups with neighbouring dipoles [17, 18]. Moreover, the asymmetric and symmetric deformations located at 1429, 1409 and 1319  $\text{cm}^{-1}$ , respectively within the characteristic O–H axial deformation region and the weakening of the bending mode at 912  $\text{cm}^{-1}$ , the SO stretching peak at 1033  $\text{cm}^{-1}$  and the symmetric CS stretch at 686  $\text{cm}^{-1}$  may be closely combined with different types of conformation of the K-DMSO composites with respect to the surface hydroxyls [14, 19]. The new peaks appeared at 3648, 3547 and 3474  $\text{cm}^{-1}$  and they were attributed to the hydroxyls of non-hy-

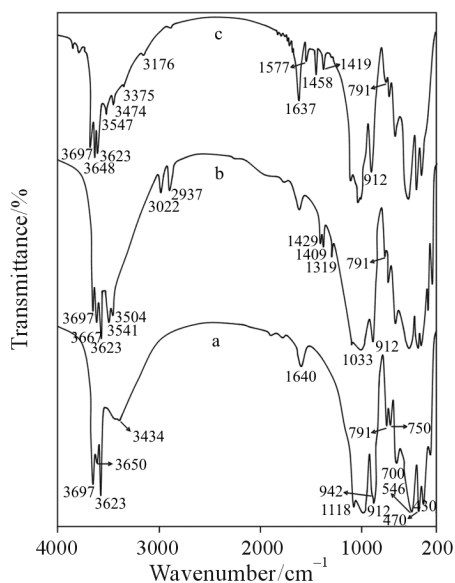


**Fig. 1** The FTIR spectra of a – raw kaolinite, b – K-DMSO composite, and c – K-Bz species

drogen bonded structural water molecules; the intensity of the mode at 3623  $\text{cm}^{-1}$  decreased significantly while the peak at 3697  $\text{cm}^{-1}$  remained unchanged following the insertion of the benzamide groups into the K-DMSO composite (Fig. 1c). Two additional N-H stretches at 3375 and 3176  $\text{cm}^{-1}$  and the striking weakening of the vibrations of siloxane layer upon deintercalation of K-DMSO which are corroborated by the intensity losses of the  $\text{Fe}^{2+}$ -OH or  $\text{Fe}^{3+}$ -OH deformation peaks at 912 and 791  $\text{cm}^{-1}$  (Fig. 1c) signify the partial removal of DMSO pre-intercalates by benzamide species. The C–N stretch at 1419  $\text{cm}^{-1}$ , the C–H deformation peak seen at 1458  $\text{cm}^{-1}$ , and the 1577  $\text{cm}^{-1}$  peak in the ring frequency region all verify that the benzamide entities were inserted into the interlamellar space in the form of an intermolecular array via the N–H group [9, 11, 20, 21].

The endothermic DTA peak of 504°C minimum with a corresponding mass loss 12.9% in the temperature interval 397–628°C on the TG curve of raw kaolinite resulted from the dehydroxylation process, whereas the sharp exothermic DTA peak at 987°C with no mass losses resembled a phase change to form  $\gamma$ -alumina and/or mullite (Fig. 2a). The K-DMSO precursor presents an endothermic peak at 164°C (temperature range: 80–203°C; mass loss: 18.24%), which can be attributed to the molecular desorption of DMSO, and the other peak at 512°C (a 13.07% mass loss) arises from dehydroxylation whereas the phase transition at 984°C was the exothermic event of the DTA profile of the K-DMSO composite, respectively (Fig. 2b). The K-Bz species presents two relatively small endothermic peaks of the maxima at 196 and 250°C (the mass losses by 9.61 and 3.86%, respectively) on the TG curve of K-Bz which are related to the gradual elimination of the Bz species and the decomposition of the organic matter, respectively, while the strong endothermic peak centred at 500°C in the range 405–537°C (a mass loss of 12.18%) corresponds to the matrix dehydroxylation process of the thermally deintercalated mineral (Fig. 2c) [22]. Since the dehydroxylation pattern of the K-Bz derivative is not significantly different from that of K-DMSO (Fig. 2b, c), it seemed that the DMSO residues that are co-distributed with the Bz entities on the interior surfaces [23] may have made interlayer diffusion more difficult and contributed to a weaker inorganic host-guest interaction. The fact that an endothermic peak was not observed in the thermal analysis of the K-Bz species near the temperature of DMSO desorption confirms the insertion of the Bz species into the ditrigonal cavity of the siloxane layer by the substitution of the pre-adsorbed DMSO composites [18]. The DMSO composites are not only required to provide access to inner surface hydroxyls

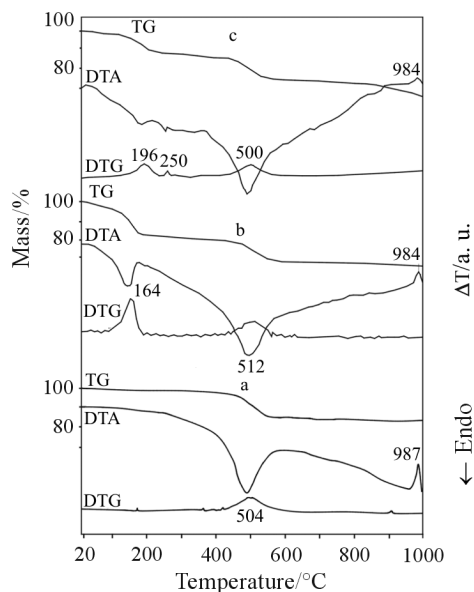


**Fig. 2** DTA, TG and DTG curves of a – raw kaolinite, b – K-DMSO composite, and c – K-Bz species

but also are directly involved in the actual chemistry and thus enhance notably the stability of the complex benzamide-kaolinite. In these interactions, the interlamellar organic groups are grafted by covalent bonds to the silicate sheets, which permits obtaining thermally and chemically more stable entities [12, 20]. The thermal stability of the K-Bz derivative can be attributed to the slightly tilted aromatic ring keying into the gibbsitic sheets via the  $-NH_2$  groups similar to those in the kaolinite-pyridine intercalation compound [19, 24].

The XRD reflections of raw kaolinite at 7.18 and 3.58 Å (Fig. 3a) correspond to the  $d$  values 001 and 002, respectively [16, 22]. New peaks appear at 11.27 and 3.76 Å at 7.84 and 23.80(2 $\theta$ ), i.e. the DMSO molecules are directly intercalated into the kaolinite interlayer space (Fig. 3b). Disappearance of the DMSO reflections and emergence of well-defined features at 6.04(2 $\theta$ ) and 11.16(2 $\theta$ ), 001 and 002 reflections with  $d$  values of 14.62 and 7.92 Å, respectively (Fig. 3c) point out that the DMSO species were substituted efficiently by benzamide molecules. Correspondingly, stronger reflections at 12.26 and 24.80(2 $\theta$ ) in the XRD profile of K-Bz derivative than those of the DMSO intercalate indicate that the K-Bz intercalates are embedded deeply within the gallery space of kaolinite. Keying of benzamide species into the inner layers resulted in an increase of  $d(001)$  value about 7.44 Å along  $c$  axis which is below the expected basal spacing of kaolinite [15]. Since the molecular size of benzamide (7.70 Å) is bigger than this value, the benzamide species has to be tilted slightly with respect to the interlayer plane [9, 25]. The structural geometry may also allow the Bz species to conform itself to give the least expansion

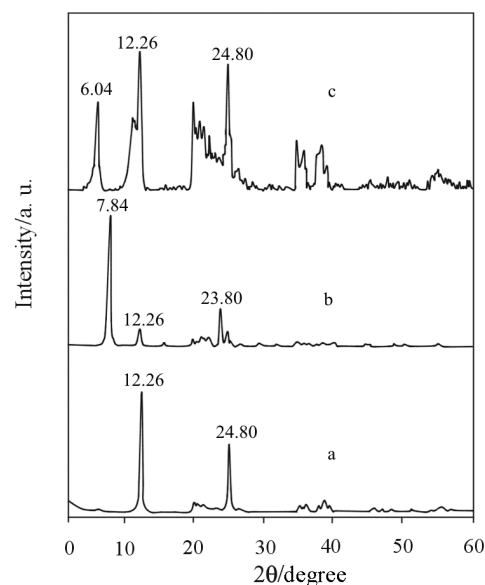


**Fig. 3** XRD patterns of a – raw kaolinite, b – K-DMSO composite, and c – K-Bz species

consistent with minimum interaction between neighbouring molecules [18]. Therefore, the smaller the size of the guest molecule the bigger the intercalation ratio as proved by the intercalation ratios of DMSO and benzamide species (80 and 40%, respectively) which were determined based upon the XRD and thermal analysis data [9]. Hence, the corresponding stoichiometry of the K-DMSO and K-Bz complexes can be given as  $Al_2Si_2O_5(OH)_4[(CH_3)_2SO]_{0.8}$  and  $Al_2Si_2O_5(OH)_4(C_6H_5CONH_2)_{0.40}$ , respectively, in agreement with the data reported in the literature [22, 26]. The still present peaks at 12.26 and 24.80(2 $\theta$ ) of kaolinite and the much smaller surface area of the K-Bz entities ( $6.62 \text{ m}^2 \text{ g}^{-1}$ ) than those of the non-intercalated kaolinite ( $12.80 \text{ m}^2 \text{ g}^{-1}$ ) and the K-DMSO composite ( $14.61 \text{ m}^2 \text{ g}^{-1}$ ) demonstrated that a significant number of the succeeding benzamide moieties are retained in the middle rather than on the edges of the clay mineral [25]. It is not surprising that the conversion of the original micropores ( $\leq 2 \text{ nm}$ ) to mesopores (2–20 nm) by the retained benzamide species primarily leads to this remarkable surface area decrease [1, 27].

## Conclusions

The FTIR spectra and thermal data reveal the presence of host-guest interactions between the K-DMSO surface and the benzamide species. The intensities of the raw kaolinite reflections at 12.26 and 24.80(2 $\theta$ ) are reduced significantly by the intercalation of the DMSO molecules. Benzamide introduction leads to a decrease in the surface area of the K-Bz composite by 45% which is concerned with the increase in particle thickness. The benzamide species inserted into the

kaolinite structure through the replacement of the K-DMSO composites remain stable up to 300°C. The DMSO composites provide access to inner surface hydroxyls and enhance notably the stability of the complex benzamide-kaolinite.

## Acknowledgements

The authors are grateful to the Research Foundation of Ondokuz Mayıs University for the financial support under the project no. F 238.

## References

- 1 G. Lagaly, *Philos. Trans. R. Soc. London, A* 311 (1984) 315.
- 2 M. Trombetta, G. Busca, M. Lenarda, L. Storaro and M. Pavan, *Appl. Catal., A*, 182 (1999) 225.
- 3 F. Bergaya and G. Lagaly, *Appl. Clay Sci.*, 19 (2001) 1.
- 4 M. J. Hernando, C. Pesquera, C. Blanco, I. Benito and F. González, *Appl. Catal.*, 141 (1996) 175.
- 5 S. Yariv, *Thermochim. Acta*, 274 (1996) 1.
- 6 H. Zhao and G. F. Vance, *Water Res.*, 32 (1998) 3710.
- 7 S. Olejnik, L. A. G. Aylmore, A. M. Posner and J. P. Quirk, *J. Phys. Chem.*, 72 (1968) 241.
- 8 J. J. Tunney and C. Detellier, *Clays Clay Miner.*, 42 (1994) 552.
- 9 J. E. Gardolinski, L. P. Ramos and G. P. Souza, *J. Colloid Interface Sci.*, 221 (2000) 284.
- 10 A. Tabak, B. Afsin, S. F. Aygun and H. Icbudak, *J. Therm. Anal. Cal.*, 81 (2005) 311.
- 11 B. K. G. Theng, *The Chemistry of Clay-Organic Reactions*, John Wiley and Sons, New York 1974, p. 243.
- 12 Y. Komori, Y. Sugahara and K. Kuroda, *J. Mater. Res.*, 13 (1998) 930.
- 13 P. M. Constanzo, C. V. Celemency and R. F. Giese, *Clays Clay Miner.*, 28 (1980) 155.
- 14 J. G. Thompson and C. Cuff, *Clays Clay Miner.*, 33 (1985) 490.
- 15 E. Horváth, J. Kristóf, R. L. Frost, A. Rédey, V. Vágvölgyi and T. Cseh, *J. Therm. Anal. Cal.*, 71 (2003) 707.
- 16 M. Raupach, P. F. Baron and J. G. Thomson, *Clays Clay Miner.*, 35 (1987) 208.
- 17 F. A. Cotton, R. Francis and W. D. Horrocks, *J. Am. Chem. Soc.*, 64 (1960) 1534.
- 18 C. T. Johnston and D. A. Stone, *Clays Clay Miner.*, 38 (1990) 121.
- 19 R. L. Ledoux and J. L. White, *J. Colloid Interface Sci.*, 21 (1966) 127.
- 20 J. J. Tunney and C. Detellier, *J. Mater. Chem.*, 6 (1996) 1679.
- 21 B. Afsin and M. Macit, *Phys. Low-Dim. Struct.*, 3/4 (1998) 191.
- 22 K. D. Pennel, R. D. Rhue and W. G. Haris, *Clays Clay Miner.*, 39 (1991) 360.
- 23 B. P. Kelleher and T. F. O'Dwyer, *Clays Clay Miner.*, 50 (2002) 331.
- 24 A. Tabak and B. Afsin, *Adsorpt. Sci. Technol.*, 19 (2001) 673.
- 25 Y. Sugahara, S. Satokawa, K. Kuroda and C. Kato, *Clays Clay Miner.*, 38 (1990) 137.
- 26 S. Yariv, I. Lapidés, K. H. Michaelian and N. Lahav, *J. Therm. Anal. Cal.*, 56 (1999) 865.
- 27 A. K. Helmy, E. A. Ferreiro and S. G. Debussetti, *J. Colloid Interface Sci.*, 210 (1999) 167.

---

Received: December 12, 2005

Accepted: November 6, 2006

---

DOI: 10.1007/s10973-005-7472-3